JOURNAL OF MATERIALS SCIENCE **36** (2001) 3793–3800

Oxidation resistance and electrical properties of silicon carbide added with Al_2O_3, AlN, Y_2O_3 and NiO

T. CHARTIER, J. M. LAURENT, D. S. SMITH
SPCTS-UMR CNRS 6638, Ecole Nationale Supérieure de Céramique Industrielle, 47 à 73 avenue Albert Thomas, 87065 LIMOGES Cedex, France
E-mail: t.chartier@ensci.fr

F. VALDIVIESO, P. GOEURIOT, F. THEVENOT
Ecole Nationale Supérieure des Mines de Saint-Etienne, Centre SMS, 158, cours Fauriel, 42023 SAINT-ETIENNE Cedex 2, France

Because of its excellent thermal, mechanical and electrical properties silicon carbide is widely used for heating elements. Nevertheless these elements are affected by electrical ageing (increase of electrical resistivity during use). This phenomenon is generally attributed to oxidation but no satisfactory answer has been presently found to reduce its effects. The aim of this study is to obtain a better understanding of the degradation of the electrical properties through the oxidation behavior of hot pressed samples containing various amount of additives. Eight dense SiC ceramic samples with Al_2O_3, AlN, Y_2O_3 and NiO additives were prepared by hot pressing. The influence of these additives on sintering, oxidation behavior and electrical properties was evaluated. Formation of an yttrium garnet phase leads to liquid phase sintering but decreases the oxidation resistance. The dependence of electrical resistivity with temperature can be explained by the presence or not of a metallic phase formed between Ni and Si. This secondary phase permits a low ($<5\ \Omega \cdot$cm) and almost constant value of the electrical resistivity from ambient temperature up to 950°C to be obtained.

1. Introduction

Since a long time, silicon carbide has widely been used as a heating element between 1200 and 1600°C because of its good mechanical and electrical properties. Nevertheless, electrical ageing of SiC constitutes the major drawback of its application at high temperature in oxidizing environment. The main parameters which influence the electrothermal behavior have recently been reviewed for SiC commercial heating elements [1] constituted of α-SiC, β-SiC or $(\alpha+\beta)$-SiC. The grain size varied from 100 μm to 300 μm depending on the major polytype and the porosity was approximately 30 vol. %. This high value of porosity will promote oxidation which is usually considered as responsible for electrical ageing [2]. The second origin of the ageing could be attributed to the nature of the secondary phases, depending on the type and on the amount of additives contained in the elements [3].

As a complementary approach this paper examines the thermal stability and the electrical behaviour of dense SiC ceramics (with less than 2 % porosity) containing various amounts of Al_2O_3, AlN, Y_2O_3 and NiO additives. These additives are generally used in the processing of silicon carbide materials because of their ability to enhance electrical and structural properties.

2. Experimental

2.1. Starting materials

A commercial α-SiC powder (FCP 13 Norton, U.S.A.) with an average grain size of 1.5 μm was used. Its chemical characteristics are given in Table I.

Because of the highly covalent character of the Si-C bond, silicon carbide can not be sintered without using high pressure and/or the presence of sintering additives to form a liquid phase. A classical way is to use Al_2O_3 and Y_2O_3 additives to promote the formation of the yttrium aluminum garnet (YAG) phase which allows liquid phase sintering of SiC between 1760 and 2000°C [4]. SiC materials exhibiting 99% or more of the theoretical density can then be achieved [5]. In this respect, additives were Al_2O_3 (Baïkowski, France, $d_{50}=0.50\ \mu$m), AlN (Atochem, France, $d_{50}=1\ \mu$m) and Y_2O_3 (Rhone Poulenc, France, $d_{50}=1.1\ \mu$m). NiO (Prolabo, France, $d_{50}=0.5\ \mu$m) was used to obtain suitable electrical properties.

2.2. Preparation of samples

The samples composition was chosen using one half fraction of a 2^k factorial design [6]. The value of k was fixed by the number of additive powders (the number of

TABLE I Chemical analysis of the silicon carbide powder used

Chemical analysis of the Norton FCP 13 SiC powder					
Free SiO_2 (%)	0.8	Fe (ppm)	100	Cr (ppm)	10
Free Si (%)	0.03	Al (ppm)	600	Ca (ppm)	40
Free C (%)	0.25	Ni (ppm)	10	Ti (ppm)	100
		V (ppm)	120	Mg (ppm)	<100
		Na (ppm)	200		

TABLE II Composition of the samples prepared according to the 2^{k-1} factorial design (wt. % with respect to SiC powder)

Sample	Al_2O_3 (wt %)	AlN (wt %)	Y_2O_3 (wt %)	NiO (wt %)
I	0.5	0.5	0.5	0.5
II	0.5	5	5	0.5
III	5	5	0.5	0.5
IV	0.5	0.5	5	5
V	5	0.5	5	0.5
VI	0.5	5	0.5	5
VII	5	5	5	5
VIII	5	0.5	0.5	5

experiments was then equal to $2^{4-1} = 8$). Each weight concentration of additive was taken to a minimum (0.5 wt. %) or to a maximum value (5 wt. %). Table II presents the eight compositions used in this study. For all compositions, the SiC powder and the additives were mixed with ethanol in a zirconia ball mill for one hour, then dried in air at 85°C for at least 3 hours. After this operation, the mean grain size of the powder mix was approximately 0.6 μm.

Powder pellets, with a diameter of 50 mm and a height of 10 mm, were formed by dry pressing with a low pressure ($P = 4$ MPa) in a graphite die and then were subjected to hot pressing under 40 MPa in argon. A temperature of 1800 °C was chosen to achieve densification with less than 2 % of residual porosity. The sintering time and the final density for each sample are reported in Table III. Hot pressing presents the advantage that evaporation of additives during sintering is lowered compared to pressureless sintering.

2.3. Characterisation

The influence of the nature and of the amount of additives was studied in terms of i) microstructure of sintered samples, ii) phases developed during sintering, iii) oxidation behaviour and, iv) electrical properties.

The density of the hot pressed samples was measured using Archimede's method. Secondary phase formation in the hot pressed samples was investigated by X-ray diffraction. Observations of the sample microstructures were performed after a fine polishing of the surfaces and an palsma-etching. Secondary phases and oxide layers (formed after oxidation treatment) were performed using a scanning electron microscope coupled with an energy dispersive spectrometer. Samples were polished and the microstructures were revealed by plasma etching. All the oxidation experiments were conducted on the hot pressed samples in a way that the real conditions of use for the heating elements were approached. They were oxidized under static air at 1000 °C, 1200 °C and 1400 °C in a furnace containing an inside layer of a silico- aluminate refractory. These temperatures were attained using a heating rate of 60 $^{\circ}C \cdot min^{-1}$. The weight gains were measured after short treatment periods (1 to 2 hours) in the early stage of oxidation and then every 10 or 20 hours.

Electrical resistivity was measured on hot pressed samples from room temperature to 950 °C in air, using the four terminal method in order to avoid any electrical contact resistance [7]. The voltage (U) between two terminals separated by a distance l is measured on a sample crossed by a direct current (I) applied between two other terminals separated by a distance $L(L > l)$. For a given temperature, the electrical resistivity is obtained from the relation:

$$\rho = (U/I) \times (S/l) \quad (1)$$

were S is the cross section of the element.

TABLE III Sintering time and density of hot pressed samples (1800°C − 40 MPa)

Sample	Sintering time (min)	Density ($g \cdot cm^{-3}$)
I (0.5 wt % Al_2O_3; 0.5 wt % AlN; 0.5 wt % Y_2O_3; 0.5 wt % NiO)	30	3.23
II (0.5 wt % Al_2O_3; 5 wt % AlN; 5 wt % Y_2O_3; 0.5 wt % NiO)	15	3.28
III (5 wt % Al_2O_3; 5 wt % AlN; 0.5 wt % Y_2O_3; 0.5 wt % NiO)	40	3.34
IV (0.5 wt % Al_2O_3; 0.5 wt % AlN; 5 wt % Y_2O_3; 5 wt % NiO)	20	3.34
V (5 wt % Al_2O_3; 0.5 wt % AlN; 5 wt % Y_2O_3; 0.5 wt % NiO)	10	3.27
VI (0.5 wt % Al_2O_3; 5 wt % AlN; 0.5 wt % Y_2O_3; 5 wt % NiO)	40	3.20
VII (5 wt % Al_2O_3; 5 wt % AlN; 5 wt % Y_2O_3; 5 wt % NiO)	15	3.34
VIII (5 wt % Al_2O_3; 0.5 wt % AlN; 0.5 wt % Y_2O_3; 5 wt % NiO)	2	3.28

3. Results and discussion

3.1. Densification and microstructure of samples

All hot pressed samples show a very high density 3.20 to 3.34 $g \cdot cm^{-3}$ and do not present open porosity (Table III). Because it is not easy to accurately determine the theoretical density for each composition, values of relative density were not calculated. The SEM micrograph (Secondary electron image) of samples I, V and VII which contain 2, 11 and 20 wt% of additives are presented in Figs 1–3, respectively. These three micrographs are representatives of the size of SiC grains after sintering, according to the amount of the additives (samples II, III, IV, VI, and VIII are similar to sample VII). The grain size is decreasing when the amount of additives is increasing. The large grey zones correspond to the SiC matrix, white and black zones correspond to YAG-rich and Ni-rich intergranular phases, respectively. SEM observations and Energy dispersive analysis on samples reveals, i) a continuous grain boundary second phase with a high level of yttrium and aluminum (example of sample IV in Fig. 4) and, ii) the presence of crystallized grains containing nickel and silicon (example of sample IV in Fig. 5), approximately 1 μm in size, located at grain boundary in the intergranular second phase for samples containing 5 wt % NiO (sample IV, VI, VII, VIII). No porosity was observed. It clearly appears that the grain growth is not important, the grain size stays roughly equal or lower to one micrometer. Grain growth is inhibited when the quantity of additives is large.

X-Ray diffraction experiments on samples containing 5 wt% Al_2O_3 and 5 wt % Y_2O_3 (samples V, VII) confirms the presence of the YAG (example of sample V in Fig. 6). In the case of samples containing a low amount of Al_2O_3, i.e. 0.5 wt %, 5 wt % AlN and 5 wt % Y_2O_3 (sample II), the formation of the YAG phase was also expected but surprisingly the only detected secondary phase is the yttrium silicate Y_2SiO_5.

3.2. Oxidation of the hot pressed samples

3.2.1. $T = 1000\,^{\circ}C$

Oxidation experiments on the hot pressed samples were first conducted at 1000 °C. For all the compositions, in our weight gain detection range ($\Delta m > 0.1$ mg) no weight change could be recorded after 80 hours of treatment in static air at this temperature. This is not surprising if we consider that the formation of a 1 μm thick amorphous oxide scale (density 2.2) on our samples would represent a weight gain of 0.07 mg. Several studies report the oxidation of pure SiC and mention weight gain as low as 0.3 $mg \cdot cm^{-2}$ after 100 hours of treatment at 1300°C in wet air [8] or layer thickness as thin as 0.1 μm after 40 hours of treatment at 1100°C in dry air [9]. The absence of detectable weight change for our samples at 1000°C suggests a very slow rate of surface oxidation and that our additives containing samples behave in a manner similar to pure SiC. At 1000 °C, no crystallization of the oxide layer could be detected by small angle X-ray diffraction. We can then assume the formation of an amorphous oxide scale (such SiO_2, characterized by large amount of Si by EDS analysis), through passive oxidation of the hot pressed samples. This behavior is generally encountered at low

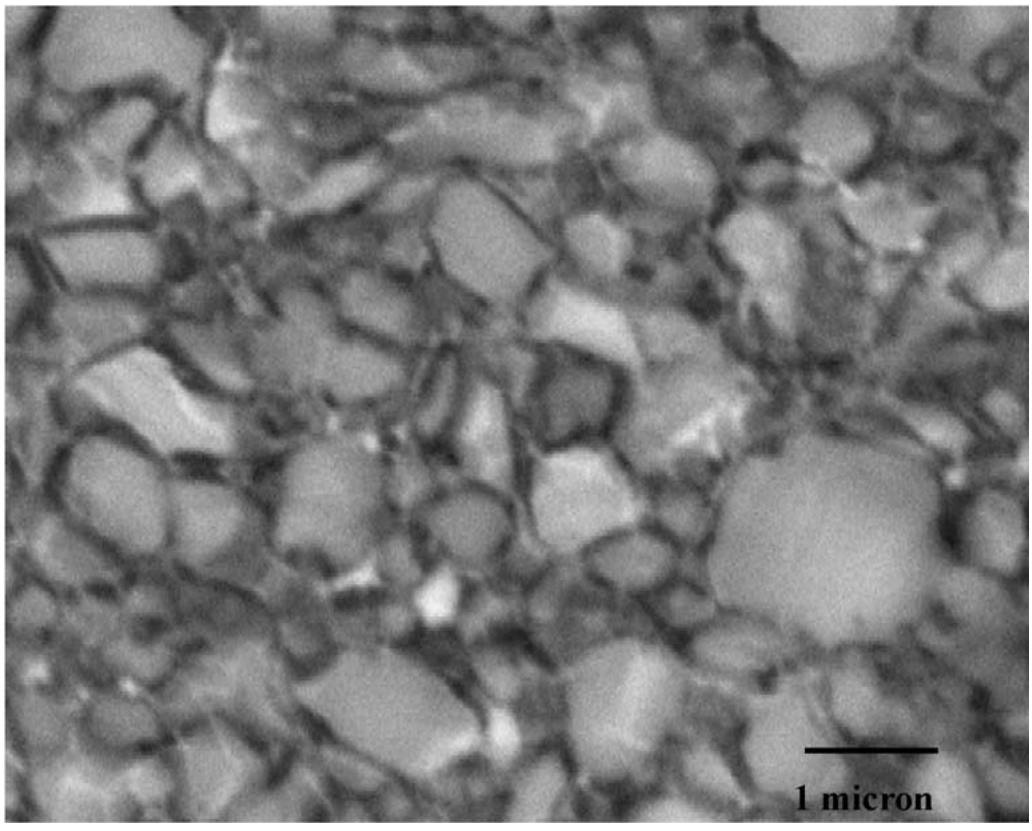

Figure 1 SEM micrograph of sample I (0.5 wt % Al_2O_3; 0.5 wt % AlN; 0.5 wt % Y_2O_3; 0.5 wt % NiO). Grey zone corresponds to the SiC matrix, white and black zones correspond to the YAG-rich and Ni-rich intergranular phases, respectively.

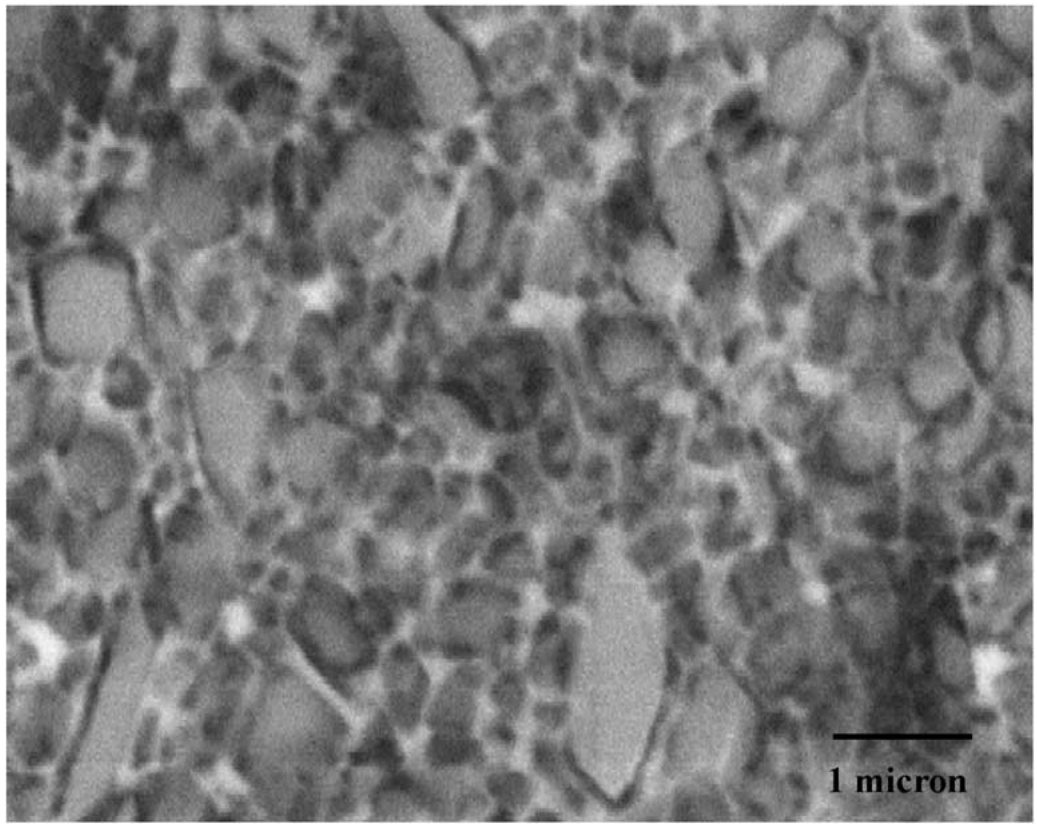

Figure 2 SEM micrograph of sample V (5 wt % Al_2O_3; 0.5 wt % AlN; 5 wt % Y_2O_3; 0.5 wt % NiO). Grey zone corresponds to the SiC matrix, white and black zones correspond to the YAG-rich and Ni-rich intergranular phases, respectively.

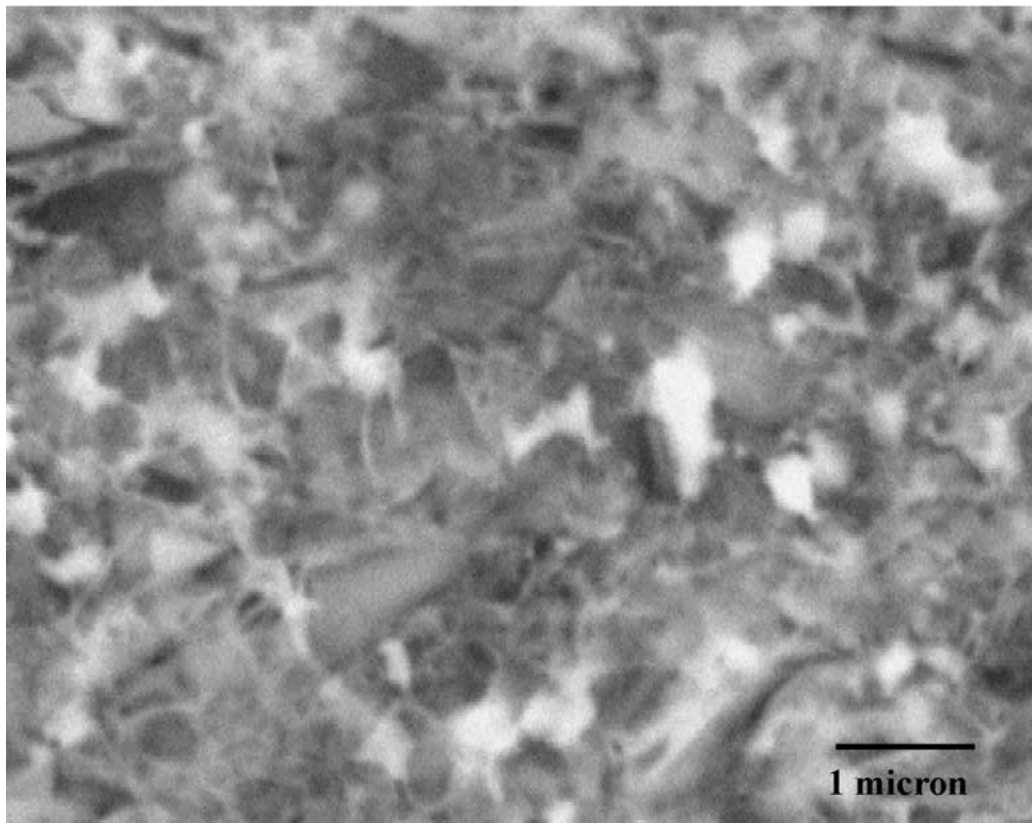

Figure 3 SEM micrograph of sample VII (5 wt % Al_2O_3; 5 wt % AlN; 5 wt % Y_2O_3; 5 wt % NiO). Grey zone corresponds to the SiC matrix, white and black zones correspond to the YAG-rich and Ni-rich intergranular phases, respectively.

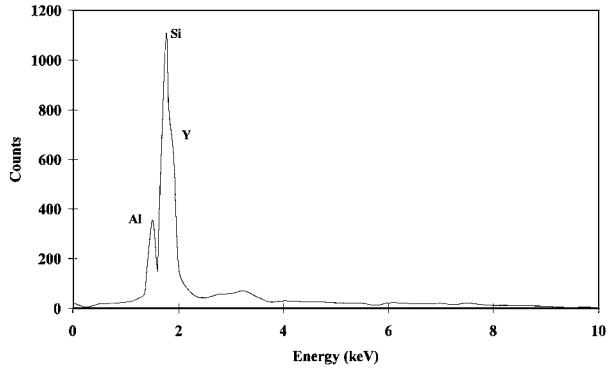

Figure 4 Energy Dispersive Analysis of the grain boundary phase of sample IV (0.5 wt % Al_2O_3; 0.5 wt % AlN; 5 wt % Y_2O_3; 5 wt % NiO).

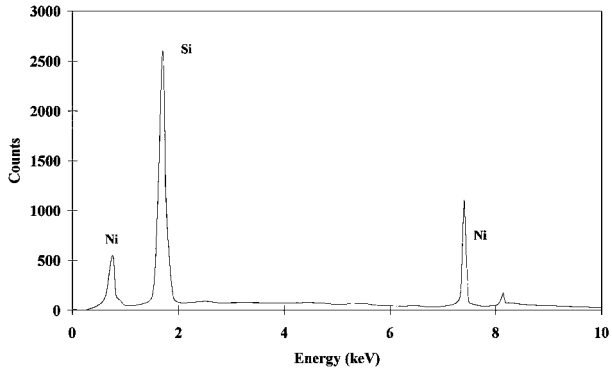

Figure 5 Energy Dispersive Analysis of the crystallized secondary phase present in sample IV (0.5 wt % Al_2O_3; 0.5 wt % AlN; 5 wt % Y_2O_3; 5 wt % NiO).

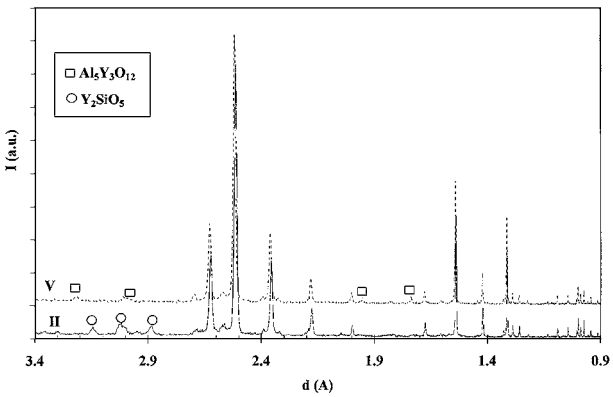

Figure 6 X-Ray diffraction patterns of sample II (0.5 wt % Al_2O_3; 5 wt % AlN; 5 wt % Y_2O_3; 0.5 wt % NiO) and sample V (5 wt % Al_2O_3; 0.5 wt % AlN; 5 wt % Y_2O_3; 0.5 wt % NiO).

temperature and high oxygen pressure. The rate controlling reactions are as follows (depending on the local equilibrium) [9, 10]:

$$SiC + O_2 \leftrightarrow SiO_2 + C \quad (2)$$

$$SiC + 3/2\,O_2 \leftrightarrow SiO_2 + CO \quad (3)$$

$$SiC + 2\,O_2 \leftrightarrow SiO_2 + CO_2 \quad (4)$$

The passive oxidation mechanism favors the formation of an amorphous or crystallized (depending on the temperature and/or impurity contained in the material) protective surface layer which develops by oxygen diffusion to the SiC/SiO_2 interface.

3.2.2. $T = 1200$ and $1400\,^{\circ}C$

In comparison to the oxidation treatments conducted at 1000 °C, the weight gain increases at higher temperatures for all compositions, consequently the oxidation rate because the dimensions of the samples, and surfaces exposed to oxidation, are identical. The weight gain is an order of magnitude higher at 1400 °C than at 1200°C (Figs 7 and 8). This result strongly differs from the oxidation behavior of pure silicon carbide or of pure silicon nitride above 1100 °C as was described by Billy [10]. This author and others [11–15] reported decreasing oxidation rates with increase of temperature in the range 1100 °C–1500 °C, attributed to the crystallization of the protective surface SiO_2 layer which occurs above 1100 °C and is promoted at higher temperatures. This is clearly not the case in our study. At 1400°C after 10 hours of treatment the oxidation is stopped, suggesting a protective surface layer, whereas at 1200°C the weight gain is continuous, even after 60 hours. The oxidized layer at 1200°C is likely not enough thick to prevent from oxidation. In addition, the secondary phases, which depend on the nature and on the amount of additives, have a significant influence on oxidation of doped SiC materials [3, 16–18].

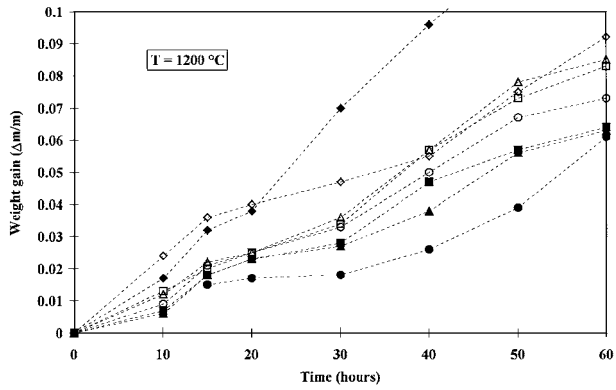

Figure 7 Weight gain evolution versus time at 1200 °C for the eight hot pressed samples □ Sample I, △ Sample II, ◇ Sample III, ○ Sample IV, ■ Sample V, ▲ Sample VI, ◆ Sample VII, ● Sample VIII.

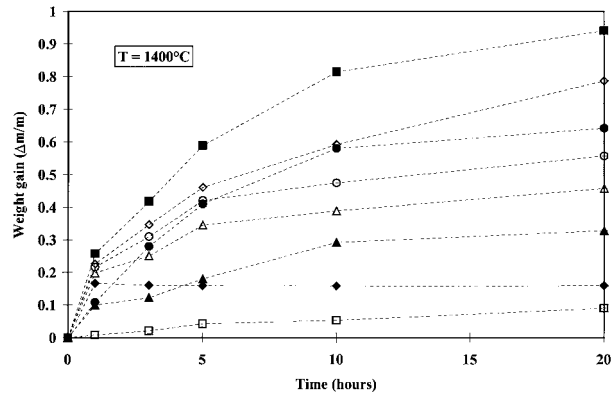

Figure 8 Weight gain evolution versus time at 1400 °C for the eight hot pressed samples □ Sample I, △ Sample II, ◇ Sample III, ○ Sample IV, ■ Sample V, ▲ Sample VI, ◆ Sample VII, ● Sample VIII.

3.2.3. Influence of the quantity of additives

A satisfactory interpretation of our results can be related to the sample composition. In general, for a given temperature, increased dopant concentrations lead to higher oxidation rates [16]. The origin of this phenomenon can be explained by the generated chemical gradient between the pure SiO_2 growing layer at the surface of the ceramic body and the additives and impurities cations containing silicate, in the grain boundary of the silicon carbide material [19]. This gradient induces the migration of metal cations, from the grain boundary formed during the sintering stage, towards the growing oxide scale. As a result, the viscosity of the growing silica layer is even further reduced since the oxidation temperature and then cation migration are high. In the case of our doped SiC samples, a temperature increase corresponds to an increased flow of oxygen towards the SiC/SiO_2 interface and consequently to an enhanced reaction between SiC and O, that increases the growing rate of the surface oxide layer as shown by samples VII and I at 1200 °C and 1400 °C (Figs 7 and 8).

After 30 hours of oxidation at 1200 °C, sample VII, which contains the highest total proportion of additives, exhibits the fastest weight gain whereas, for the other samples, the weight gain values are difficult to separate, taking into account the accuracy of the weight measurement (Fig. 7).

In contrast, sample I (lowest total amount of additives) clearly exhibits the best oxidation resistance (Fig. 8) confirming the advantage of minimizing the amount of additives.

3.2.4. Influence of the nature of the additives

Apart from the specific case of sample VII, it can be noted that the other samples containing 5 wt. % of Al_2O_3 (sample III, V and VIII) exhibit the highest rates of oxidation at 1400°C. This may be explained by diffusion of aluminum through the oxide scale since this cation is known to lower the oxide scale viscosity [12, 16, 19]. An EDS analysis reveals the abundant presence of Al and Y in the oxide scale formed at the surface of samples V, and in all samples which contain a high amount of Y_2O_3, Al_2O_3 or AlN. Yttrium silicate crystals formed by migration of yttrium cations into the scale after oxidation treatment of sample V at 1400 °C are clearly visible (Fig. 9). Nevertheless, depending on the origin of this cation (Al_2O_3 or AlN), a noticeable difference exists between the oxidation behaviors of the aluminum containing samples. The better oxidation resistance of sample II (0.5 wt. % Al_2O_3; 5 wt. % AlN; 5 wt. % Y_2O_3; 0.5 wt. % NiO) compared to sample V (5 wt. % Al_2O_3; 0.5 wt. % AlN; 5 wt. % Y_2O_3; 0.5 wt. % NiO) is evident. The YAG phase was not detected in sample II (§ 3.1.), whereas this phase was present in sample V. A study concerning the oxidation of Al-doped SiC mentions a better oxidation resistance when Al originates from AlN rather than from Al_2O_3 [7]. This suggests that the presence of the YAG phase was detrimental to the oxidation resistance of SiC.

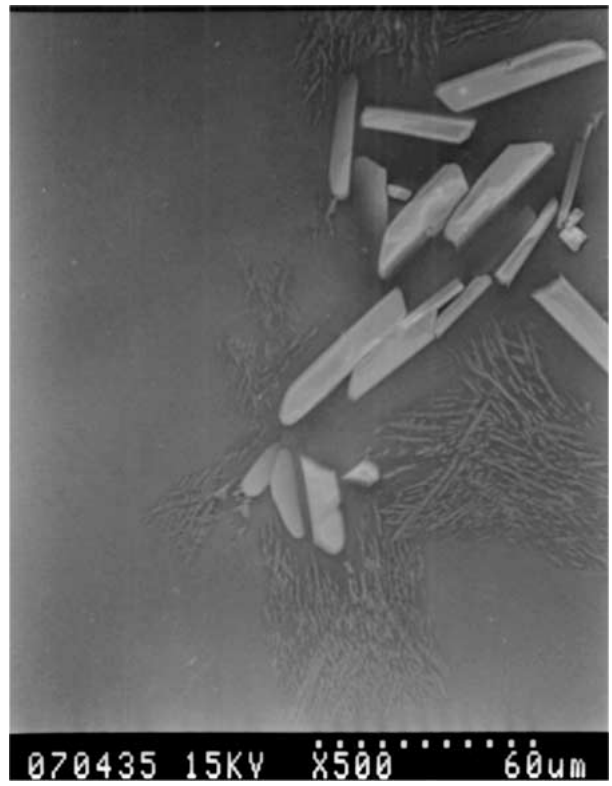

Figure 9 SEM micrography of sample V showing yttrium silicate crystals in the SiO_2 scale.

As we have seen in Figs 1 to 3 the microstructure of samples I, V and VII are very different. To quantify the chemical composition of oxidized layer, a comparison of the migration of cations (additives and impurities) between sample I (low amount of additives) and samples V and VII (high amount of additives) treated at 1200 in air, with a hold time of 10 and 40 hours, has been performed by EDS semi-quantitative analysis on the outer surface of the oxidized layer. At this temperature, the quantities of impurities increase in the oxide layer as the time increase. Concerning the impurities, we can not conclude on the evolution of their concentration versus time in the oxide layer because their concentrations in the oxide layer are under the limit of detection of the acquisition system (1 wt.%).

3.2.5. Influence of cycling

A cycling procedure from 20 °C to the oxidation treatment temperature was used to evaluate the oxidation resistance of our materials. The weight gain was measured on samples taken out of the furnace and then inserted again for a further oxidation time. This method can have an influence on the results. As an example, the effect of cycling on Al_2O_3 doped SiC has already been considered as responsible for occurrence of cracks. Nevertheless, it was shown that the cracks immediately heal during the next cycle and that the final obtained oxidation behavior is very similar to an isothermal oxidation treatment [20]. The oxidation rate is also similar during oxidation without cycling.

An advantage of the cycling can be the break down of the oxidation kinetics into several stages. From the representation of the square of the weight gain versus time

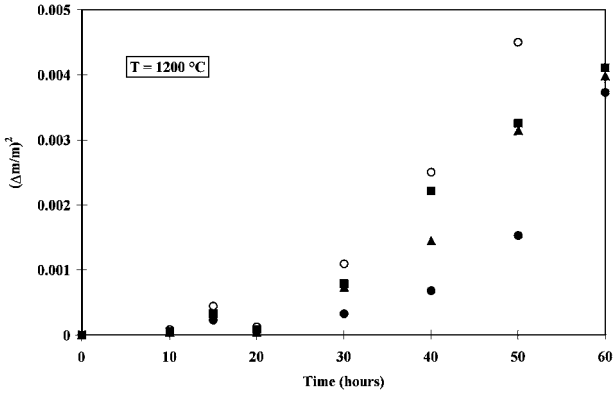

Figure 10 Variation of the square of the weight gain (in percentage) with time at 1200 °C. Samples IV(○), V(■), VI(▲) and VIII(●).

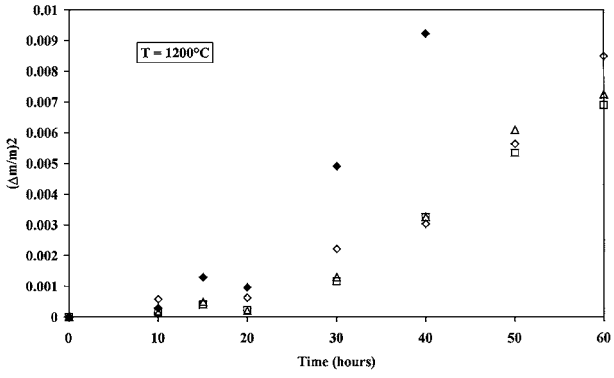

Figure 11 Variation of the square of the weight gain (in percentage) with time at 1200 °C. Samples I(□), II(△), III(◇) and VII(◆).

(Figs 10 and 11) at 1200 °C, it can be seen that an increase of the oxidation rate occurs after about 20 hours of treatment. These increase can be attributed to the microstructural and composition modifications of the oxide layer due to the migration of additives.

3.2.6. Conclusions

From this study on the oxidation of doped HP SiC samples, three major conclusions can be retained; i) the lowest amount of additives promotes the best oxidation resistance (note the low oxidation rate of sample I) and the highest quantity of additives leads to the least desirable oxidation behavior (note the high oxidation rate of sample VII at 1200°C); ii) the presence of the YAG phase seems to decrease the resistance to oxidation and the nature of the additives is of major importance (note the better oxidation behavior obtained with AlN compared to Al_2O_3 addition); iii) apart from sample I (lowest amount of additives) oxidation rates do not follow simple parabolic law especially at 1400 °C due to the modification of the properties of the protective oxide layer by outward migration of additives.

3.3. Electrical properties

Fig. 12 shows the electrical resistivity variation from room temperature to 950°C for the hot-pressed samples. Two groups of results can be distinguished. The first group is constituted of samples containing 5 wt %

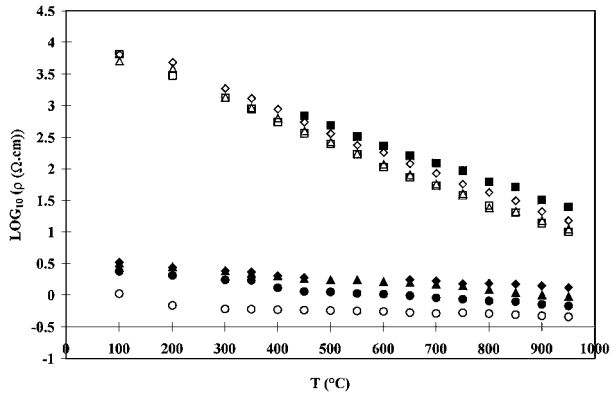

Figure 12 Variation of the electrical resistivity with temperature for the hot pressed samples. Samples I(□), II(△), III(◇), IV(○), V(■), VI(▲), VII(◆) and VIII(●).

of NiO with a rather constant value of resistivity in the range 20 °C–950 °C. The second group consist of the four samples with 0.5 wt. % of NiO displaying a constant decrease of the resistivity with temperature. At room temperature, the electrical resistivity of the second group samples is lying around 8000 $\Omega \cdot$ cm and for the first group it is comprised between 1 and 5 $\Omega \cdot$ cm showing the determinant role of NiO on the samples resistivity. The increase of the resistivity generally reported from around 700°C to higher temperatures for silicon carbide [21] is not observed for our materials. The electrical behaviour of our samples, of particularly relevance to heating elements, are obtained through the combination of different effects. When a small amount of NiO is present (0.5 wt %), the variation of ρ versus T is quite similar to the results obtained for pure SiC crystals [21]. However, in the case of a large amount of NiO (5 wt. %), the low and almost constant value of the resistivity in the range of temperature studied almost certainly indicates the presence of a metallic type component which might be Ni_3Si_2 as suggested by the elementary analysis performed on grains present at the grain boundary (§ 3.1 – sample IV containing 5 % NiO). This type of secondary phase has already been encountered by Hashiguchi [22]. Its resistivity is approximately $10^{-4}\Omega \cdot$ cm at room temperature with a metallic type behaviour up to 750 °C.

When the data of electrical conductivity is plotted in an Arrhenius diagram (Fig. 13), it can also be noted that

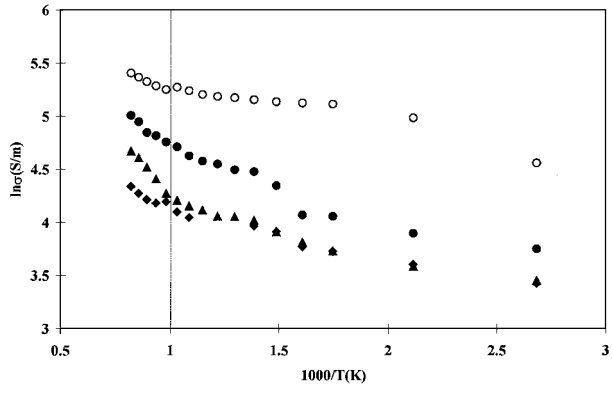

Figure 13 Electrical conductivity variation of the four samples containing high level of nickel oxide. Samples IV(○), VI(▲), VII(◆) and VIII(●).

for the four samples containing 5 wt. % NiO there is a steepening of the apparent activation energy to greater than 0.1 eV above 700 °C. This suggests that the metal phase grains no longer act as a complete bypass of the SiC grains.

4. Conclusion

Silicon carbide samples containing different combinations of four additives (Al_2O_3, AlN, Y_2O_3 and NiO) have been analyzed in terms of oxidation behavior and electrical resistivity. The nature of the additives present at their high level in the samples were determinant for the four characteristics listed above.

The association of alumina or aluminum nitride to yttrium oxide clearly favored the appearance of a liquid phase at a temperature above 1600°C and consequently the densification. The Al_2O_3/Y_2O_3 combination leads to the formation of the YAG phase. When aluminum nitride was used instead of alumina the YAG phase was no longer detected.

The oxidation resistance of the eight hot pressed samples was good, especially at 1000°C where no weight gain could be measured after 80 hours of treatment. At 1200°C, the oxidation was still very slow but after about 20 hours of treatment, an acceleration of the weight gain, probably correlated with impurity and additives cations diffusion toward the reaction interface, in the surface SiO_2 protective scale, was recorded. At 1400°C, whatever the composition, the samples appeared to be less resistant to oxidation than at 1000 and 1200 °C. In particular, the samples containing high levels of alumina and yttrium oxide exhibited less oxidation resistance while those samples with lowest additive content reacted more slowly.

Formation of a metallic type phase Ni_3Si_2 decreased electrical resistivity of the samples containing a high level of NiO (5 wt. %). The resistivity was also almost constant in the range of temperature tested, i.e. from 20 °C to 950 °C which is very interesting for the heating element application of silicon carbide.

This electrical behavior associated with a good oxidation resistance should allow the performance of silicon carbide heating elements to be improved.

Acknowledgments

The authors thank Mrs M. Le Boulch and Mr R. Jaume (EDF, Direction des Etudes et Recherches, Service AEE, Département ADEI, BP. 1, route de Sens, 77250 Moret sur Loing, France) for their technical and financial support.

References

1. K. PELISSIER, T. CHARTIER and J. M. LAURENT, *Ceram. Int.* **24** (1998) 371.
2. A. E. S. WHITE and A. NORCOTT, *British Ceram. Soc. Proceedings* (1968) 141.
3. S. C. SINGHAL and F. F. LANGE, *J. Amer. Ceram. Soc.* **58**(9/10) (1975) 433.
4. M. A. MULLA and V. D. KRSTIC, *Ceram. Bull.* **70**(3) (1991) 439.
5. S. JIHONG, G. JINGKUN and J. DONGLIANG, *Ceram. Int.* **19** (1993) 347.
6. D. C. MONTGOMERY, "Design and Analysis of Experiments," 3rd ed. (John Wiley and Sons Inc., New-York, 1991).
7. J. F. BAUMARD, "Compendium of Thermophysical Property Measurement Methods" Vol. 1, edited by K. D. Maglié, A. Cezarairliyan and V. E. Peletsky (Plenum Press, New-York, 1984) p. 271.
8. M. MAEDA, K. NAKAMURA and M. YAMADA, *J. Amer. Ceram. Soc.* **72**(3) (1989) 512.
9. C. E. RAMBERG, G. CRUCIANI, K. E. SPEAR and R. E. TRESSLER, *ibid.* **79**(11) (1996) 2897.
10. M. BILLY, *Mat. Sc. Eng.* **88** (1987) 53.
11. M. A. LAMKIN, F. L. FILEY and R. J. FORDHAM, *J. Eur. Ceram. Soc.* **10** (1992) 347.
12. E. OPILA, *J. Amer. Ceram. Soc.* **78**(4) (1995) 1107.
13. R. E. TRESSLER, "Corrosion Advanced Ceramics," edited by K. G. Nickel (Kluwer Academic Press, The Netherlands, 1994) p. 3.
14. K. L. LUTHRA, *J. Amer. Ceram. Soc.* **74**(5) (1991) 1095.
15. D. S. FOX, *ibid.* **81**(4) (1998) 945.
16. J. A. COSTELLO and R. E. TRESSLER, *ibid.* **69**(9) (1986) 674.
17. S. C. SINGHAL, *J. Mater. Sci.* **11** (1976) 1246.
18. D. BAXTER, A. BELLOSI and F. MONTEVERDE, *J. Eur. Ceram. Soc.* **20** (2000) 367.
19. N. S. JACOBSON, *J. Amer. Ceram. Soc.* **76**(1) (1993) 3.
20. M. MAEDA, K. NAKAMURA, T. OHKUBO, J. ITO and E. ISHII, *Ceram. Int.* **15** (1989) 247.
21. W. D. KINGERY, H. K. BOWEN and D. R. UHLMAN, "Introduction to Ceramics," 2nd ed. (J. Wiley and Sons, USA, 1976).
22. H. HASHIGUCHI and H. KINUGASA, *J. Ceram. Soc. Jap.* **102**(2) (1994) 160.
23. F. K. VAN DIJEN and E. MAYER, *J. Eur. Ceram. Soc.* **16** (1996) 413.
24. J. F. LI and R. WATANABE, *J. Ceram. Soc. Jap.* **102**(8) (1994) 727.
25. L. CORDREY, D. E. NIESZ and D. J. SHANEFIELD, *Ceram. Trans.* **7** (1990) 618.
26. T. NARHUSHIMA, T. GOTO, Y. IGUSHI and T. HIRAI, *J. Amer. Ceram. Soc.* **74**(10) (1991) 2583.
27. P. GOURSAT, P. GOEURIOT and M. BILLY, *Mat. Chem.* **2** (1976) 31.

Received 14 October 1999
and accepted 1 February 2000